

to appear in Ap.J. Letters, Aug. 20, 1996

The $^{12}\text{C}/^{13}\text{C}$ Isotopic Ratio in Photodissociated Gas in M42

R. T. Boreiko and A. L. Betz

Center for Astrophysics and Space Astronomy, University of Colorado, Boulder, CO 80309

ABSTRACT

We have observed the $158\ \mu\text{m}\ ^2\text{P}_{\frac{3}{2}} \leftarrow ^2\text{P}_{\frac{1}{2}}$ fine-structure line of $^{12}\text{C}\ \text{II}$ simultaneously with the $F = 2 \leftarrow 1$ and $F = 1 \leftarrow 0$ hyperfine components of this transition in $^{13}\text{C}\ \text{II}$ in the Orion photodissociation region near $\theta^1\text{C}$. The line profiles were fully resolved using a heterodyne spectrometer with $0.5\ \text{km s}^{-1}$ resolution. The relative intensities of these lines give a $^{12}\text{C}/^{13}\text{C}$ isotopic ratio of $R = 58\ (^{+6}_{-5})$ for the most probable $^{12}\text{C}\ \text{II}$ peak optical depth $\tau = 1.3$. The constrained range of $\tau(^{12}\text{C}\ \text{II})$ between 1.0 and 1.4 corresponds to a range of $^{12}\text{C}/^{13}\text{C}$ between 52 and 61. The most probable value of 58 agrees very well with that obtained from a relationship between the isotopic ratio and galactocentric distance derived from CO measurements, but is lower than the specific value of 67 ± 3 obtained for Orion from CO data. An isotopic ratio as low as 43, as previously suggested based on optical absorption measurements of the local interstellar medium, is excluded by the C II data at about the 2σ level.

Subject headings: ISM:abundances, infrared:ISM:lines, line:profiles, ISM:individual:M42

1. Introduction

The $^{12}\text{C}/^{13}\text{C}$ isotopic ratio of the interstellar medium is believed to be an important parameter for tracing the chemical evolution of the galaxy. ^{12}C is a primary product of stellar nucleosynthesis because it can be formed in first generation, metal-poor stars, while ^{13}C is a secondary product. Thus, through successive cycles of star formation, nucleosynthesis, and enrichment of the interstellar medium with processed material, the $^{12}\text{C}/^{13}\text{C}$ ratio is expected to decrease with time, eventually reaching a steady-state value near 4. The solar system ratio of ~ 89 is thought to be representative of the interstellar medium approximately 5 billion years ago, while the present ratio can serve as a useful check on models of galactic evolution.

The $^{12}\text{C}/^{13}\text{C}$ isotopic ratio in the Orion region has previously been measured using the isotopomers of many different molecules, yielding values between 24 and 83, often not overlapping at the 1σ level. The data prior to 1980 have been summarized by Wannier (1980), who finds a

formal abundance ratio from these data of 60 ± 8 . Radio spectra of CH_3OH , OCS , HC_3N , and the ^{13}C variants of these molecules have been observed in Orion by Johansson et al. (1984), who deduced an isotopic ratio near 40. Langer and Penzias (1990) found a relationship between the $^{12}\text{C}/^{13}\text{C}$ ratio and galactocentric distance from $^{13}\text{C}^{18}\text{O}$ and $^{12}\text{C}^{18}\text{O}$ spectra, but their measured ratio of 67 ± 3 in Orion is much higher than would be expected on the basis of this relationship. As pointed out by all these authors, estimating the isotopic ratio from relative intensities of molecular lines is subject to uncertainty because of the possibilities of chemical fractionation, self-shielding effects from photodissociating radiation, and line saturation of the more abundant isotope. At the lower radio frequencies, contamination by lines from other species is not inconsequential at the small signal levels entailed in measurements of rare isotopomers, especially in the chemically rich Orion IRc2 region. In addition, uncertainties in relative calibration and pointing when spectra are not obtained simultaneously can lead to significant systematic errors.

In this Letter, we describe well-resolved observations of the $^{12}\text{C II } ^2\text{P}_{\frac{3}{2}} \leftarrow ^2\text{P}_{\frac{1}{2}}$ fine-structure transition and the $F = 2 \leftarrow 1$ and $F = 1 \leftarrow 0$ hyperfine components of the corresponding $^{13}\text{C II}$ line near $\theta^1\text{C}$ in the Orion photodissociation region. Since these data were obtained simultaneously, there is no systematic uncertainty caused by pointing differences or absolute calibration of individual spectra. Furthermore, since all of the carbon within the PDR is in the form of C^+ , interpretation of the measured line intensity ratio to derive the isotopic ratio is relatively straightforward.

2. Instrumentation and Calibration

The data were obtained using a far infrared heterodyne receiver (Betz and Boreiko 1993) flown onboard the Kuiper Airborne Observatory (KAO). The local oscillator (LO) is an optically pumped CH_2F_2 laser operating at 1891.2743 GHz (Petersen, Scalabrin, and Evenson 1980), 9.3 GHz away from the rest frequency of the $^{12}\text{C II}$ line at 1900.5369 GHz (Cooksy, Blake, and Saykally 1986). The mixer is a GaAs Schottky diode (University of Virginia type 1T11) in a corner-reflector mount. Both the mixer and the first intermediate frequency (IF) amplifier are cooled to 77 K. The system noise temperature measured during the observations was 9500 K single sideband (SSB). The IF signal is analyzed by a 400-channel acousto-optic spectrometer (AOS), with a channel resolution of 3.2 MHz (0.5 km s^{-1}) and a usable bandwidth of 150 km s^{-1} at the C II frequency.

The observations were done using sky chopping at 2.2 and 4.4 Hz, with an amplitude of $9/4$ in 1990 and $12/5$ in 1991, respectively. These chop amplitudes are sufficient to ensure little emission in the reference beam in the NE-SW chop direction (see the map of Stacey et al. 1993). The reduction in peak intensity from off-source emission is at most 10% if there is no velocity gradient in the source, and it is smaller if the emission in the two reference beams occurs at a different peak LSR velocity from that in the main beam. The C II spectra obtained in 1990

and 1991 had different reference beam locations because of differences in both chop amplitude and position angle; thus, the excellent agreement between line profiles provides further evidence that contamination from off-source emission is not a significant source of uncertainty for these observations. Any residual contamination would affect both isotopes similarly, and therefore to first order, the derived isotopic ratio should be unaffected if the optical depth in the ^{12}C II line is not much greater than 1 (see section 4).

The telescope beam size was $43''$ (FWHM) and the pointing accuracy is estimated to be $\sim 15''$. Absolute intensity calibration is derived from spectra of the Moon, for which a physical temperature of 394 K and emissivity of 0.98 are adopted (Linsky 1973). Conversion from double sideband (DSB) to SSB intensity was performed using the calculated transmission of the atmosphere in the two sidebands, corrected for the different source and lunar elevation angles. The observed signals are quoted as T_r^* , the antenna temperature corrected for all factors except the coupling of the source to the beam (Kutner and Ulich 1981). The net calibration uncertainty for a source filling the beam is $\leq 15\%$. The velocity scale accuracy, determined from the known line and LO rest frequencies, is better than $\pm 0.15 \text{ km s}^{-1}$ (1σ).

3. Observations

The C II line was observed from the KAO flying at an altitude of 12.5 km on the nights of 1990 Dec 11 and 1991 Oct 30, Nov 1, and Nov 2. Data were obtained at several locations near $\theta^1\text{C}$ in M42. All the observations were within $35''$ of the position of peak C II emission seen in the map of Stacey et al. (1993), which is approximately $20''$ SW of $\theta^1\text{C}$. The variation in peak intensity between spectra is $\leq 10\%$, in agreement with that expected from the C II map. There is, however, a pronounced velocity gradient over the range covered by our observations, with the C II line at $\theta^1\text{C}$ redshifted by 1.6 km s^{-1} relative to that $45''$ west. No comparable gradient is seen in the north - south direction, with peak V_{LSR} changing by less than 0.2 km s^{-1} over $40''$. There is also a significant change in line profile between the $\theta^1\text{C}$ spectrum and that seen $45''$ further west, with the former being wider and having a $\sim 10\%$ contribution to the total integrated intensity from a distinct velocity component characterized by $V_{\text{LSR}} = 0.8 \text{ km s}^{-1}$, and the latter showing a somewhat asymmetric profile with an extended red wing.

All the spectra from positions with integrated intensity above the 90% of peak contour from the map of Stacey et al. (1993) were averaged, yielding a net spectrum with an integration time of 162 minutes. The corresponding uncertainty per 0.50 km s^{-1} channel is 0.37 K (1σ). The spectrum includes two of the three ^{13}C II hyperfine components: $F = 2 \leftarrow 1$ and $F = 1 \leftarrow 0$, at velocities of $+11 \text{ km s}^{-1}$ and -65 km s^{-1} relative to the ^{12}C II velocity (Cooksy, Blake, and Saykally 1986). These two components contain 80% of the total ^{13}C II fine-structure line intensity. The $F = 1 \leftarrow 1$ hyperfine line containing the remaining 20% was outside the bandwidth of the present observations.

The $F = 1 \leftarrow 0$ $^{13}\text{C II}$ hyperfine line is well-isolated from the $^{12}\text{C II}$ line, and therefore its intensity can be determined directly. However, the $F = 2 \leftarrow 1$ component is superposed on the wing of the $^{12}\text{C II}$ line. Therefore, we fitted the red wing of the $^{12}\text{C II}$ 158 μm line, excluding the region around the $^{13}\text{C II}$ $F = 2 \leftarrow 1$ frequency, to a sum of Gaussian profiles, to the statistical uncertainty of the data. This wing profile was then subtracted from the spectrum, leaving the desired $^{13}\text{C II}$ hyperfine component. Figure 1 shows an expanded view of the data and the fit that was subtracted. No physical significance is attached here to the three velocity components used in the fit.

The frequencies for the hyperfine components were refined from the data by assuming that their velocities agree with that of the $^{12}\text{C II}$ line. The resulting apparent LSR velocities are $11.6 \pm 0.2 \text{ km s}^{-1}$ to the red and $64.5 \pm 0.4 \text{ km s}^{-1}$ to the blue of the $^{12}\text{C II}$ line for the $F = 2 \leftarrow 1$ and $F = 1 \leftarrow 0$ components respectively, in agreement with those given by Cooksy et al. (1986) to within 1σ . The spectral regions surrounding the $F = 2 \leftarrow 1$ and $F = 1 \leftarrow 0$ $^{13}\text{C II}$ lines were placed on the correct V_{LSR} scales and coadded. The resulting $^{13}\text{C II}$ spectrum is shown in Figure 2. The T_r^* scale has been multiplied by 1.25 to account for the missing $F = 1 \leftarrow 1$ component and therefore represents the corrected antenna temperature that would have been measured if all the $^{13}\text{C II } ^2\text{P}_{\frac{3}{2}} \leftarrow ^2\text{P}_{\frac{1}{2}}$ fine-structure radiation had been observed.

Table 1 presents various parameters of the observed spectra. The peak T_r^* , V_{LSR} , and width for the $^{12}\text{C II}$ line are derived from a Gaussian fit to the line between 5.6 km s^{-1} and 10.2 km s^{-1} V_{LSR} , since this narrow part of the line can adequately be described by a Gaussian profile and appears uncontaminated by other velocity components. The parameters for the $^{13}\text{C II}$ transitions come from fits to the entire lines. For the $^{13}\text{C II}$ $F = 2 \leftarrow 1$ component, all the parameters are determined after subtraction of the wing of the $^{12}\text{C II}$ line. Velocity limits for the integrated intensity are $\Delta v(\text{FWHM})$ on either side of line center for the $^{13}\text{C II}$ hyperfine components. However, the limits for the $^{12}\text{C II}$ line are -5 km s^{-1} to $+25 \text{ km s}^{-1}$, in order to include the broad low-intensity emission. The integrated intensity attributable to the $^{13}\text{C II}$ $F = 2 \leftarrow 1$ component has been subtracted. Note that the integrated intensity for the $^{12}\text{C II}$ line therefore has a significant contribution from velocity components other than the main narrow feature at $V_{\text{LSR}} \sim 8.4 \text{ km s}^{-1}$, and there is some broad wing emission beyond the velocity range used for the calculation.

4. Analysis and Interpretation

The ratio of peak intensities for the $^{12}\text{C II}$ and $^{13}\text{C II}$ lines gives the $^{12}\text{C}/^{13}\text{C}$ isotopic ratio directly only if both lines are optically thin. Models of photodissociation regions suggest that the $^{12}\text{C II}$ line near $\theta^1\text{C}$ has a small to moderate optical depth with $\tau \lesssim 1$ (Tielens and Hollenbach 1985a, 1985b). Stacey et al. (1991) detected the $^{13}\text{C II}$ $F = 1 \leftarrow 0$ transition and mapped its integrated intensity over a small region near $\theta^1\text{C}$. These authors calculated a $^{12}\text{C II}$ line-averaged optical depth $\tau_{av} = 0.75 \pm 0.25$ in the inner region of the nebula (including the immediate vicinity

of $\theta^1\text{C}$) and $\tau_{av} \sim 3$ for our observed location. However, these values depend upon an adopted $^{12}\text{C}/^{13}\text{C}$ isotopic ratio of 43.

Boreiko, Betz, and Zmuidzinas (1988) observed the $F = 2 \leftarrow 1$ hyperfine component and derived an optical depth for the ^{12}C II line near $\theta^1\text{C}$ of 5.6 ± 1.7 using an adopted $^{12}\text{C}/^{13}\text{C}$ isotopic ratio of 60. These earlier data had a considerably lower signal-to-noise ratio and somewhat lower spectral resolution than those presented here, and the $F = 2 \leftarrow 1$ transition was detected only at the 3σ level. While the line position, width, and peak ^{12}C II intensity observed by Boreiko, Betz, and Zmuidzinas (1988) are in good agreement with those shown in Table 1, the earlier value for the peak intensity of the ^{13}C II transition is almost a factor of 2 higher, possibly because of inadequate subtraction of the extended wing of the ^{12}C II line. The two data sets are in agreement at the 1.5σ level, although the difference corresponds to a significant variation in derived optical depth.

Because gas densities in the $\theta^1\text{C}$ region are known to be at least 10^5 cm^{-3} , the optical depth of the ^{12}C II line can be determined directly if the kinetic temperature of the emitting gas is known. The $63 \mu\text{m } ^3P_1 - ^3P_2$ fine-structure line of O I also arises from photodissociated gas, and it is optically thick in models of the Orion PDR (Tielens and Hollenbach 1985b). Boreiko and Betz (1996) fully resolved the O I and C II lines at $\theta^1\text{C}$, and they modeled their peak intensities to give a kinetic temperature for the photodissociation region of 175 K - 220 K, with a “best-fit” value of 185 K. The uncertainty in the temperature arises mainly from the unknown density of the region, since the O I line may be subthermally excited. The optical depth of the ^{12}C II line was found to be between 1.0 and 1.3, with a most likely value of 1.2.

If the kinetic temperature at the observed location is assumed to be the same as that at $\theta^1\text{C}$ ($\sim 40''$ further east from the centroid of observations), then the optical depth of ^{12}C II is somewhat higher, 1.0 - 1.4, with a most likely value of 1.3. This is consistent with the data of Stacey et al. (1991), which show lower optical depth near the center of the H II region surrounding $\theta^1\text{C}$. The $^{12}\text{C}/^{13}\text{C}$ isotopic ratio R can be calculated from the observed ^{12}C II/ ^{13}C II *peak* intensity ratio:

$$R = \frac{-\tau_{12}}{\ln[1 - \frac{I_{13}}{I_{12}}(1 - e^{-\tau_{12}})]}. \quad (1)$$

For a peak optical depth $\tau_{12} = 1.3$ for the ^{12}C II line, the relative ^{12}C II and ^{13}C II peak intensities of Table 1 give a $^{12}\text{C}/^{13}\text{C}$ isotopic ratio of $58 (\pm 6)$, where the limits show 1σ statistical uncertainty. The possible range of τ_{12} between 1.0 and 1.4, determined from the uncertainty in the derived temperature of the PDR, corresponds to a range of $^{12}\text{C}/^{13}\text{C}$ between 52 and 61, with the same statistical uncertainty.

The relative widths of the ^{12}C II and ^{13}C II lines provide supporting information on the optical depth of the ^{12}C II line. Since the beamsize and pointing were identical for all the observed transitions, the $\sim 20\%$ difference in FWHM can be ascribed to optical depth broadening of the ^{12}C II line. The line profiles are assumed to be described by a Gaussian in column density and hence in optical depth. The intrinsic width is assumed to be the same for the ^{12}C II and ^{13}C II

lines, while their peak optical depths τ_{12} and τ_{13} differ by a factor of R , the isotopic ratio. This factor R does not enter into the calculation of relative widths from optical depth broadening. Using line width data only, $\tau_{12} = 1.1$ ($^{+0.9}_{-0.7}$), in good agreement with the $\tau_{12} = 1.3$ value derived independently from peak-intensity data. Spectrally resolved observations of the hyperfine ^{13}C II transitions with a higher signal-to-noise ratio would be valuable in obtaining a more precise value of the optical depth of the ^{12}C II line, and, therefore, also for the $^{12}\text{C}/^{13}\text{C}$ ratio.

Systematic uncertainties in the kinetic temperature and peak intensity of the C II lines affect the derived isotopic ratio in a very nonlinear manner. Since the ^{12}C II and ^{13}C II components were measured simultaneously, there is no relative calibration uncertainty. However, possible self-chopping, estimated to be below the 10% level in integrated intensity, will affect the derived optical depth of the ^{12}C II line. The kinetic temperature calculated for the region remains essentially unaffected by self-chopping of C II emission. The main consequence would be an increase in the best-fit hydrogen column density and hence optical depth in the ^{12}C II, ^{13}C II, and O I lines (see Boreiko and Betz 1996). If the C II reference beam positions have 10% of the integrated intensity of the observed position, then the corrected peak ^{12}C II/ ^{13}C II intensity ratio would increase to yield an isotopic ratio of 66.

The profile of the ^{12}C II line provides an additional constraint on the magnitude of any self-chopping. Since the gas in the off-source beam is less optically thick than that in the region of interest, self-chopping (with no velocity gradient) will flatten the peak of the observed line and increase the apparent width. Fitting of a Gaussian profile with moderate optical depth to the ^{12}C II line between 5 and 11 km s^{-1} V_{LSR} , where asymmetry and other velocity components are not significant, suggests that $\tau_{12} < 1.5$. At higher τ_{12} , the reduced χ^2 of the fit exceeds 2 and makes the data incompatible with an optically thick line profile at the 90% confidence level. Thus, we can conclude that reference beam emission $\sim 10'$ from our observed location in the NE-SW chop direction (which was not sampled by the E-W scan of Stacey et al. 1993) is either below the 10% integrated intensity level or occurs at a velocity at least 1-2 km s^{-1} shifted from that of the peak of the observed line. High-resolution observations at the reference beam locations would help to reduce the remaining systematic uncertainty in the optical depth of the ^{12}C II line and hence in the $^{12}\text{C}/^{13}\text{C}$ isotopic ratio.

Our value of $^{12}\text{C}/^{13}\text{C}$ above is in excellent agreement with that obtained from the relationship of $^{12}\text{C}/^{13}\text{C}$ with galactocentric radius obtained by Langer and Penzias (1990) ($R = 57.4$ at the distance of Orion), from observations of $^{12}\text{C}^{18}\text{O}$ and $^{13}\text{C}^{18}\text{O}$. However, the agreement is not as good with their value of 79 ± 7 measured at IRc2 or 67 ± 3 about $3'$ NE of IRc2. As these authors pointed out, the high UV field in the region could enhance the apparent ratio because of self-shielding of the more abundant CO isotope, and therefore these derived values are likely to be too high. Alternatively, there could be a real difference in $^{12}\text{C}/^{13}\text{C}$ between the PDR and the dense molecular cloud cores producing the CO radiation. We obtained a weak detection of ^{13}C II emission at IRc2, but the signal to noise ratio of the spectrum is much smaller than at $\theta^1\text{C}$. Nevertheless, the derived isotopic ratio of 63 ± 22 is consistent with that at $\theta^1\text{C}$.

Optical observations of CH^+ toward nearby bright stars have been used to obtain a $^{12}\text{C}/^{13}\text{C}$ isotopic ratio of 43 ± 4 in the local interstellar medium with homogeneity at the 12% level (Hawkins and Jura 1987). However, molecular observations indicate a higher local value of 60 - 70 (Wilson and Matteucci 1992), so either there is significant local inhomogeneity or there remain large systematic sources of uncertainty in the methods used to determine the $^{12}\text{C}/^{13}\text{C}$ ratio. Our measured value in the PDR of Orion is inconsistent with the lower value of 43 at approximately the 2σ level.

We thank the staff of the Kuiper Airborne Observatory for their unfailing effort and helpfulness during all phases of flight operations. This work is supported by NASA grants NAG 2-254 and NAG 2-753.

Table 1. OBSERVED $^{12}\text{C II}$ AND $^{13}\text{C II}$ FINE-STRUCTURE LINE PARAMETERS AT $\theta^1\text{C}^{\text{a}}$

Transition	Peak T_r^* (K)	V_{LSR} (km s $^{-1}$)	Line Width (km s $^{-1}$, FWHM)	Integrated Intensity (erg cm $^{-2}$ s $^{-1}$ sr $^{-1}$)
$^{12}\text{C II } ^2\text{P}_{\frac{3}{2}} \leftarrow ^2\text{P}_{\frac{1}{2}}$	103.43(0.30)	8.44(0.01)	4.32(0.03)	$3.80(0.01) \times 10^{-3}$ ^b
$^{13}\text{C II } ^2\text{P}_{\frac{3}{2}} \leftarrow ^2\text{P}_{\frac{1}{2}} \text{ F} = 2 \leftarrow 1$	1.6(0.2)	8.9(0.2) ^c	3.2(0.5)	$3.98(0.04) \times 10^{-5}$
$^{13}\text{C II } ^2\text{P}_{\frac{3}{2}} \leftarrow ^2\text{P}_{\frac{1}{2}} \text{ F} = 1 \leftarrow 0$	0.9(0.2)	9.1(0.4) ^c	4.0(0.9)	$2.75(0.04) \times 10^{-5}$
$^{13}\text{C II}$ composite ^d	3.1(0.3)	8.4(0.2) ^e	3.6(0.4)	$8.35(0.07) \times 10^{-5}$

^aNumbers in parentheses represent 1σ statistical uncertainties.

^bIntegrated intensity includes several velocity components but not all extended emission.

^cCalculated using frequencies of Cooksy et al. (1986).

^dIncludes calculated contribution from $\text{F} = 1 \leftarrow 1$ hyperfine component.

^eComponent frequencies determined from the data, hence V_{LSR} is a defined value.

REFERENCES

- Betz, A. L., and Boreiko, R. T. 1993, in ASP Conf. Ser. 41, *Astronomical Infrared Spectroscopy*, ed. S. Kwok (San Francisco:ASP), 349
- Boreiko, R. T., and Betz, A. L. 1996, *ApJ*, 464, L83
- Boreiko, R. T., Betz, A. L., and Zmuidzinas, J. 1988, *ApJ*, 325, L47
- Cooksy, A. L., Blake, G. J., and Saykally, R. J. 1986, *ApJ*, 305, L89
- Hawkins, I., and Jura, M. 1987, *ApJ*, 317, 926
- Johansson, L. E. B., Andersson, C., Elldér, J., Friberg, P., Hjalmarson, Å, Höglund, B., Irvine, W. M., Olofsson, H., and Rydbeck, G. 1984, *A&A*, 130, 227
- Kutner, M. L., and Ulich, B. L. 1981, *ApJ*, 250, 341
- Langer, W. D., and Penzias, A. A. 1990, *ApJ*, 357, 477
- Linsky, J. L. 1973, *ApJS*, 25, 163
- Petersen, F. R., Scalabrin, A., and Evenson, K. M. 1980, *Int. J. Infrared Millimeter Waves*, 1, 111
- Stacey, G. J., Jaffe, D. T., Geis, N., Genzel, R., Harris, A. I., Poglitsch, A., Stutzki, J., and Townes, C. H. 1993, *ApJ*, 404, 219
- Stacey, G. J., Townes, C. H., Poglitsch, A., Madden, S. C., Jackson, J. M., Herrmann, F., Genzel, R., and Geis, N. 1991, *ApJ*, 382, L37
- Tielens, A. G. G. M., and Hollenbach, D. 1985a, *ApJ*, 291, 722
- Tielens, A. G. G. M., and Hollenbach, D. 1985b, *ApJ*, 291, 747
- Wannier, P. G. 1980, *ARA&A*, 18, 399
- Wilson, R. L., and Matteucci, F. 1992, *A&A Rev.*, 4, 1

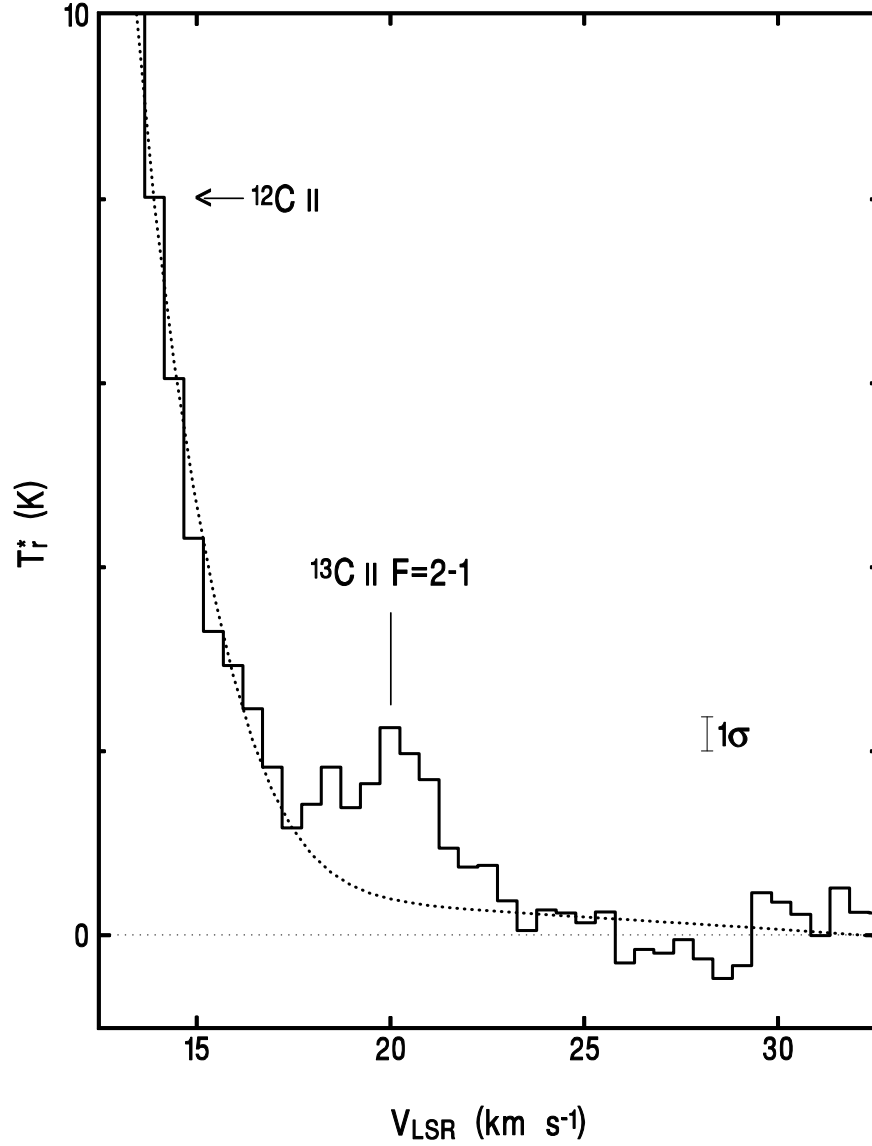


Fig. 1.— Observed spectrum of the $F = 2 \leftarrow 1$ hyperfine component of the $158 \mu\text{m } ^{13}\text{C II}$ line on the wing of the $^{12}\text{C II}$ line. The V_{LSR} scale is appropriate only for $^{12}\text{C II}$. The continuum has been removed from the spectrum. Dotted line is the fit to the $^{12}\text{C II}$ wing, which was subtracted from the data to leave only the $^{13}\text{C II}$ line.

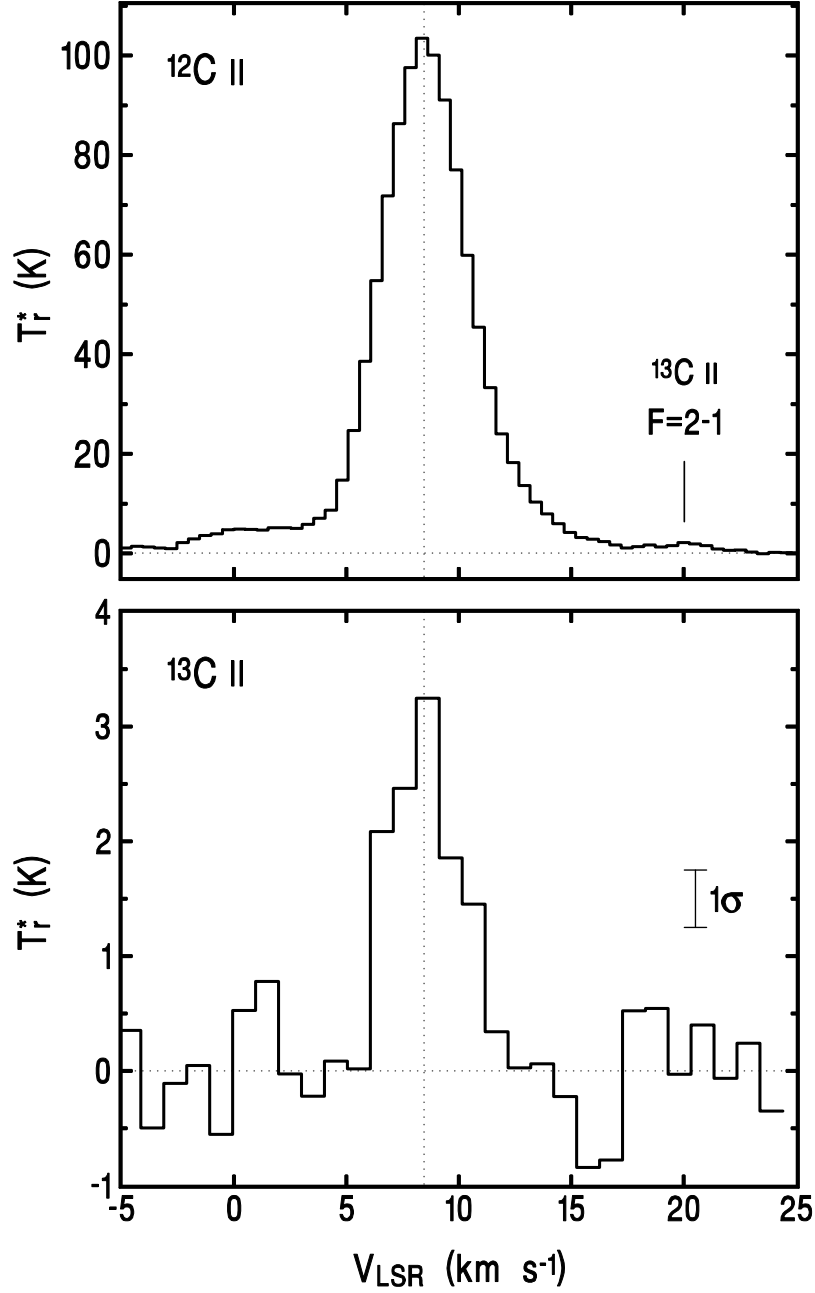


Fig. 2.— Observed spectra of the $158 \mu\text{m}$ $^{12}\text{C II}$ and composite $^{13}\text{C II}$ fine-structure lines toward $\theta^1\text{C}$ (see text for details). Integration time is 162 minutes. For the $^{12}\text{C II}$ line, 1σ is 0.37 K, too small to be clearly shown in the figure. The continuum has been removed from both spectra.